Comparison of discontinuous Galerkin and finite difference for NWP

S. Brdar*, M. Baldauf, R. Klöfkorn, A. Dedner, D.Kröner

In cooperation with DWD

We present a range of numerical tests comparing the dynamical cores of the operationally used numerical weather prediction (NWP) model COSMO and the university code DUNE, focusing on their efficiency and accuracy for solving benchmark test cases for NWP. The dynamical core of COSMO is based on a finite difference method whereas the DUNE core is based on a Discontinuous Galerkin method. Both dynamical cores are briefly introduced stating possible advantages and pitfalls of the different approaches. Their efficiency and effectiveness is investigated, based on three numerical test cases, which require solving the compressible viscous and non-viscous Euler equations. The test cases include the density current (Straka et al., 1993), the inertia gravity (Skamarock and Klemp, 1994), and the linear hydrostatic mountain waves of (Bonaventura, 2000).

The DUNE core

The DUNE dynamical core solves

$$
\begin{aligned}
\partial_t\rho + \partial_x(\rho u) + \partial_x(\rho w) &= 0,\\
\partial_t(\rho u) + \partial_x(\rho u^2 + p) + \partial_z(\rho u w) &= \partial_x(\mu\rho\partial_x u) + \partial_z(\mu\rho\partial_z u),\\
\partial_t(\rho w) + \partial_x(\rho u w) + \partial_z(\rho w^2 + p) &= -\rho g + \partial_x(\mu\rho\partial_x w) + \partial_z(\mu\rho\partial_z w),\\
\partial_t(\rho\theta) + \partial_x(\rho\theta u) + \partial_x(\rho\theta w) &= \partial_x(\mu\rho\partial_x\theta) + \partial_z(\mu\rho\partial_z\theta)
\end{aligned}
$$

in $\Omega \times [0,T]$ with $\Omega = \{(x,z)\ :\ a \le x \le b,\ f(x) \le z \le z_{top}\}$, where

$f = f(x)$	orography function,
μ	kinematic viscosity constant,
ρ and $p = p_0^{1-\gamma}(\rho R\theta)^\gamma$	density and pressure,
θ and g	potential temperature,
g	gravity constant,
γ and R	adiabatic and gas constant.

Given a tessalation $\mathcal{T}_h$ of Ω with $\cup_{K\in\mathcal{T}_h} K = \Omega$, the numerical solution $\boldsymbol{U}_h = (\rho_h, \rho_h u_h, \rho_h w_h, \rho_h\theta_h)$ is sought in $V_h^k = \{\psi \in L^2(\Omega, \mathbb{R}^4)\ :\ \psi_{|K} \in [\mathcal{P}_k(K)]^4,\ K \in \mathcal{T}_h\}$. We use the CDG2 method for spatial discretization (see [Brdar et al. 12(1)]), and strong stability Runge-Kutta (SSPRK) up to order 3 for time integration. The CDG2 method is given as

$$
\begin{aligned}
&\int_\Omega \partial_t \boldsymbol{U}_h \cdot \varphi \,\mathrm{d}x = \\
&\int_\Omega \left(\mathcal{F}(\boldsymbol{U}_h) - \mathcal{A}(\boldsymbol{U}_h, \nabla\boldsymbol{U}_h) : \nabla\varphi + S(\boldsymbol{U}_h)\cdot\varphi\right) \mathrm{d}x\\
&- \sum_{e\in\Gamma} \int_e \left(\widehat{\mathcal{F}}(\boldsymbol{U}_h) - \widehat{\mathcal{A}}(\boldsymbol{U}_h)\right) : [\![\varphi]\!]\,\mathrm{d}s\\
&+ \sum_{e\in\Gamma_i} \int_e \left(\{\!\{\mathcal{A}(\boldsymbol{U}_h)^T\nabla\varphi\}\!\} : [\![\boldsymbol{U}_h]\!] + [\![\mathcal{A}(\boldsymbol{U}_h)\nabla\boldsymbol{U}_h]\!] : [\![\varphi]\!]\right) \mathrm{d}s
\end{aligned}
$$

for all $\varphi \in V_h^k$,

with $\{\!\{\boldsymbol{V}\}\!\} = (\boldsymbol{V}^+ + \boldsymbol{V}^-)/2$, $[\![\boldsymbol{V}]\!] = (\boldsymbol{n}^+\otimes\boldsymbol{V}^+ + \boldsymbol{n}^-\otimes\boldsymbol{V}^-)$, $\mathcal{F}$ Rusanov flux, and

$$
\mathcal{A}(\boldsymbol{V})_{|e} = \begin{cases} 2\chi\left(\mathcal{A}(\boldsymbol{V}, \boldsymbol{r}_e([\![\boldsymbol{V}]\!])\right)_{K_e^-}, & \text{on } K_e^-, |K_e^-| \le |K_e^+|,\\ 0, & \text{elsewhere.}\end{cases}
$$

The lifting operator $\boldsymbol{r}_e$ is given as $\int_\Omega \boldsymbol{r}_e([\![\boldsymbol{V}]\!]) : \tau = -\int_e [\![\boldsymbol{V}]\!] : \{\!\{\tau\}\!\}$.

Well-ballancing is achieved by solving

$$
\partial_t\boldsymbol{U}' + \nabla\cdot\left(\mathcal{F}_{\text{pert}}(\boldsymbol{U}') - \mathcal{A}_{\text{pert}}(\boldsymbol{U}')\nabla\boldsymbol{U}'\right) = \mathcal{S}_{\text{pert}}(\boldsymbol{U}')
$$

assuming that the reference solution $\bar{\boldsymbol{U}}$ satisfies first PDEs with $\mu = 0$, and

$$
\begin{aligned}
\mathcal{F}_{\text{pert}}(\boldsymbol{U}') &= \mathcal{F}(\boldsymbol{U}' + \bar{\boldsymbol{U}}) - \mathcal{F}(\bar{\boldsymbol{U}}),\\
\mathcal{A}_{\text{pert}}(\boldsymbol{U}')\nabla\boldsymbol{U}' &= \mathcal{A}(\boldsymbol{U}' + \bar{\boldsymbol{U}})\nabla(\boldsymbol{U}' + \bar{\boldsymbol{U}}),\\
\hat{\mathcal{F}}_{\text{pert}}(\boldsymbol{U}') &= \hat{\mathcal{F}}(\boldsymbol{U}' + \bar{\boldsymbol{U}}) - \hat{\mathcal{F}}(\bar{\boldsymbol{U}}),\\
\hat{\mathcal{A}}_{\text{pert}}(\boldsymbol{U}')\nabla\boldsymbol{U}' &= \hat{\mathcal{A}}(\boldsymbol{U}' + \bar{\boldsymbol{U}})\nabla(\boldsymbol{U}' + \bar{\boldsymbol{U}}).
\end{aligned}
$$

Software

All simulations described here have been performed using the software packages DUNE and DUNE-FEM.

The free software package DUNE (Distributed and Unified Numerics Environment) is a modular toolbox for solving partial differential equations. It is being developed by work groups in Heidelberg, Berlin, Freiburg, and Münster (Germany), and Warwick (UK).

http://www.dune-project.org/
http://dune.mathematik.uni-freiburg.de/

DUNE-FEM is a DUNE module which defines interfaces for implementing discretization methods like Finite Element methods, Finite Volume methods, and Discontinuous Galerkin methods. In particular, DUNE-FEM features a number of parallel, locally adaptive schemes of higher order. The module is being developed in Freiburg and Münster.

The pictures and plots have been produced with ParaView and gnuplot (http://www.paraview.org/, http://www.gnuplot.info/).

References

[Baldauf 10] M. Baldauf: *A linear solution for flow over mountains and its comparison with the COSMO model.* COSMO-Newsletter 9, 19–24 (2008)

[Bonaventura 00] L. Bonaventura: *A semi-implicit semi-Lagrangian scheme using the height coordinate for a nonhydrostatic and fully elastic model of atmospheric flows.* J. Comput. Phys. 158, 186–213 (2000)

[Brdar et al. 12] S. Brdar, M. Baldauf, A. Dedner, R. Klfkorn: *Comparison of dynamical cores for NWP models.* Theor. Comput. Fluid. Dyn., DOI 10/1007/s00162-012-0264-z (2012).

[Brdar et al. 12] S. Brdar, A. Dedner, R. Klfkorn: *Compact and stable Discontinuous Galerkin methods for convection-diffusion problems.* SIAM J. Sci. Comput. 34(1), pp. 263–282 (2012).

[Colonius 04] T. Colonius: *Modeling artificial boundary conditions for compressible flow.* Ann. Rev. Fluid Mech. 36, 315–345 (2004).

[Hu 04] F. Q. Hu: *Absorbing boundary conditions (a review).* J. Comput. Fuild. Dyn. 18(6), 513-522 (2004).

[Skamarock and Klemp 94] W. C. Skamarock, J. B. Klemp: *Efficiency and accuracy of the Klemp-Wilhelmson time-splitting technique.* Mon. Weather Rev. 122, 2623–2630 (1994)

[Straka et al. 93] J. M. Straka, R. B. Wilhelmson, L. J. Wicker, J. R. Anderson, K. K. Droegemeier: *Numerical solution of a non-linear density current: a benchmark solution and comparison.* Int. J. Numer. Methods Fluids 17, 1–22 (1993)

Contact

Slavko Brdar, slavko@mathematik.uni-freiburg.de

Michael Baldauf, Michael.Baldauf@dwd.de

Andreas Dedner, A.S.Dedner@warwick.ac.uk

Robert Klöfkorn, robertk@mathematik.uni-stuttgart.de

Dietmar Kröner, dietmar@mathematik.uni-freiburg.de

MetStröm

Acknowledgment The presented results have been carried out under the support of the priority program MetStröm 1276 "Multiple Scales in Fluid Mechanics and Meteorology" of the German Research Foundation (DFG).

The COSMO core

The COSMO dynamical core solves

$$
\begin{aligned}
\partial_t u + u\partial_x u + w\partial_z u &= -\frac{1}{\rho}\partial_x p' + \frac{1}{\rho}\nabla\cdot\mathrm{T}_u,\\
\partial_t w + u\partial_x w + w\partial_z w &= -\frac{1}{\rho}\partial_z p' - g\frac{\rho'}{\rho} + \frac{1}{\rho}\nabla\cdot\mathrm{T}_w,\\
\partial_t p' + u\partial_x(\bar{p} + p') + w\partial_z(\bar{p} + p') &= -\gamma p(\partial_x u + \partial_z w),\\
\partial_t T' + u\partial_x(\bar{T} + T') + w\partial_z(\bar{T} + T') &= -(\gamma - 1)T(\partial_x u + \partial_z w)\\
&\quad -\frac{1}{c_p\rho}\nabla\cdot\mathrm{J}_s,
\end{aligned}
$$

where the diffusion fluxes T_u, T_w, and J_s are corresponding to the diffusion fluxes in the DUNE equations.

Table 1. Brief overview of the two cores.

	COSMO	
Spatial scheme	FD FD-CD (2nd order for fast) FD-UP (5th order for slow)	DG (6th order)
Temporal scheme	semi-implicit RK (2nd order)	explicit RK (3rd order)
Equation set	non-conservative Euler for p, $\vec{v}$, T	conservative Euler for ρ, $\rho\vec{v}$, $\rho\theta$
Grid	Arakawa-C	struct. □
Stabilization	artificial 4th order	Rusanov flux
Artif. bnd.	$\tau(\vec{x}) = \frac{\tau_c}{2} - \frac{\tau_c}{2}\cos\left(\pi\frac{x - x_s}{x_e - x_s}\right)$ (see [1])	

Test cases

Mountain waves

We observe the impact of single isolated hill on a horizontal wind in a neutrally stratified atmosphere (see [Bonaventura 00]). The orography is 'Witch of Agnesi' hill, $f(x) = h_m/(1 + (x/a)^2)$ with the hill height $h_m = 1$ m and the hill half-length $a = 16\,000$ m. A very accurate solution can be constructed due to relatively small hill height (see [Baldauf 10]). The governing equation are integrated until 86 000 s, by which the flow became stationary. The domain is $[100, 400]$ km $\times$ $[0, 10]$ km, and the extended domain (see below) is $[0, 500]$ km $\times$ $[0, 20]$ km.

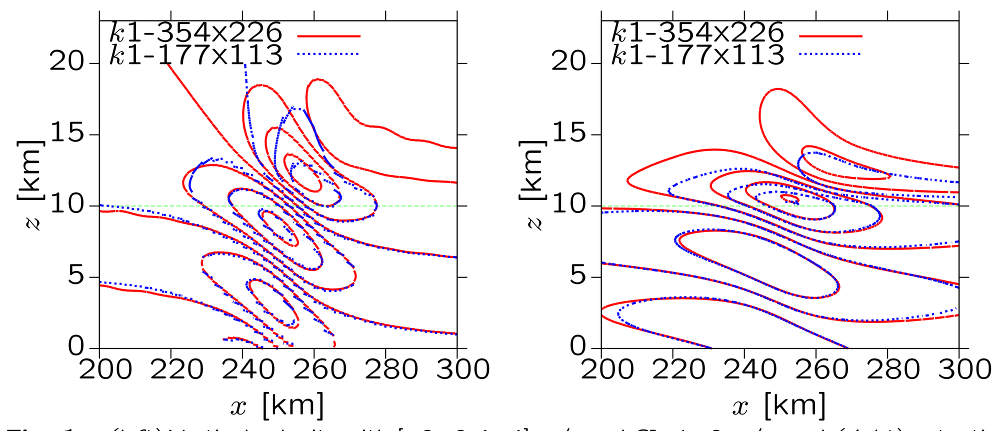

Fig. 1. *(left)* Vertical velocity with $[-3\text{e-}3, 4\text{e-}4]$ m/s and CI=1e-3 m/s; and *(right)* potential temperature with $[-0.025, 0.017]$ K and CI=7e-3 K with $\tau_c = 1/160$ for $\Delta x = 1631$ m (k1-177×113) and $\tau_c = 1/40$ for $\Delta x = 815$ m (k1-354×226).

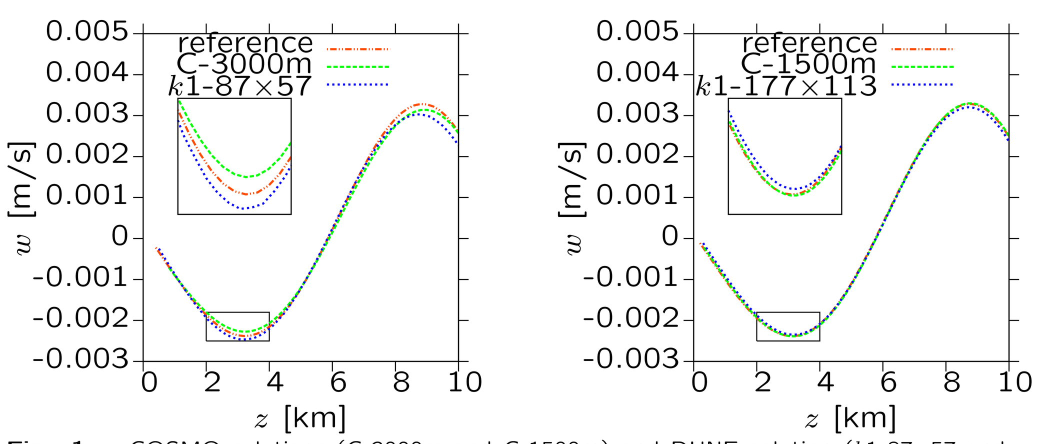

Fig. 1. COSMO solutions (C-3000m and C-1500m) and DUNE solution (k1-87×57 and k1-177×113) of the vertical velocity at *(left)* $\Delta x = 3\,000$ m and $\Delta z = 200$ m with $\tau_c = 0.1$; and *(right)* $\Delta x = 1\,500$ m and $\Delta z = 100$ m with $\tau_c = 0.025$;

Treatment of artificial boundary

A mayor difficulty of mountain wave test case is accurate treatment of artifical boundaries. Out of several techniques for treatment of such boundaries (see [Colonius 04] and [Hu 04]) we choose sponge layer technique. Our governing equations of the form

$$
\partial_t U + \nabla\cdot\mathcal{F}(U) = \mathcal{S}(U) \quad \text{in } \Omega \times (0, T)
$$

are now solved on an extended domain $\Omega_2 \times (0, T)$, where a damping function is introduced to gradually force any deviation from the reference solution towards 0. The new governing equation become

$$
\partial_t U + \nabla\cdot\mathcal{F}(U) = \mathcal{S}(U) - \tau(U - \bar{U}) \quad \text{in } \Omega_2 \times (0, T).
$$

The damping function $\tau = \tau(x)$ is taken as in Table 1.

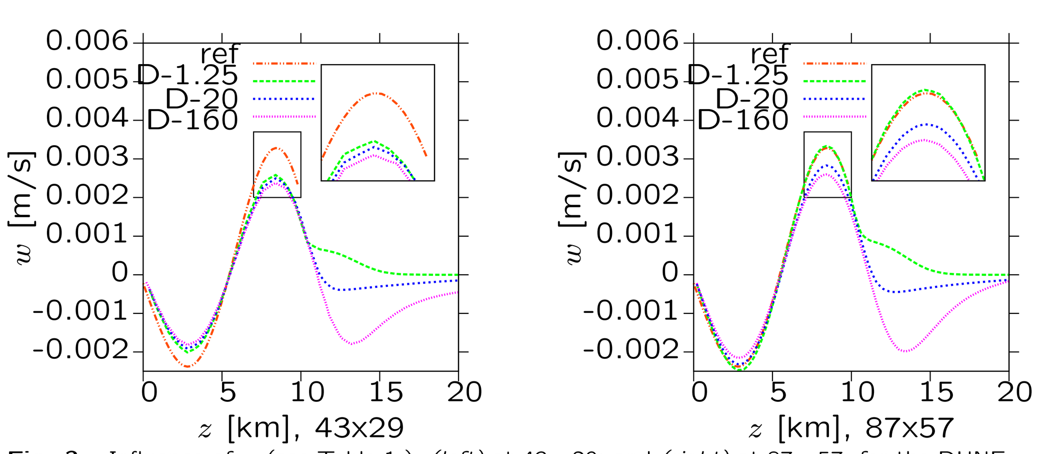

Fig. 3. Influence of τ_c (see Table 1.), *(left)* at 43 × 29; and *(right)* at 87 × 57; for the DUNE solution in comparison to the reference solution. We use $D - \tau_c$ in the legend.

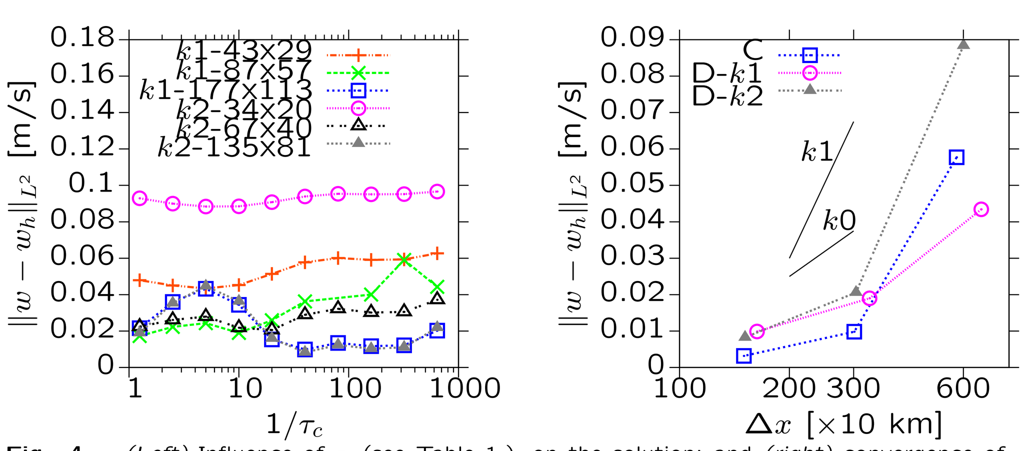

Fig. 4. *(Left)* Influence of τ_c (see Table 1.) on the solution; and *(right)* convergence of DUNE (D-k1 and D-k2) and COSMO (C).

Density current

We observe the evolution of a cold bubble in a neutrally stratified atmosphere (see [Straka et al. 93]) The bubble is introduced by perturbing the potential temperature smoothly from 0 K at the border of the bubble, to 15 K in the center. The cold bubble falls, splashes on the ground and slides along the ground level, creating Kelvin-Helmholz vortices. The governing equation are integrated until 900 s. The kinematic viscosity of 75 m²/s is introduced to obtain grid converged solution.

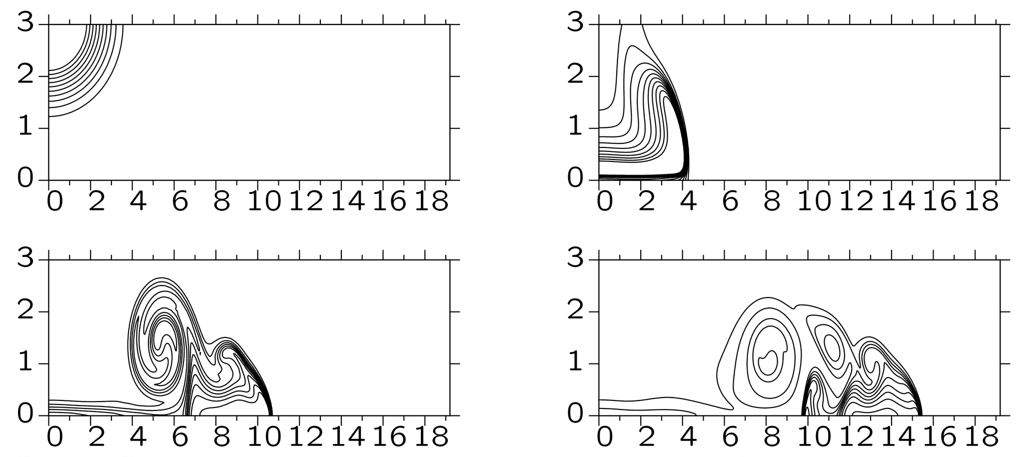

Fig. 5. Evolution of the density current at times $t = 0, 300, 600, 900$ s.

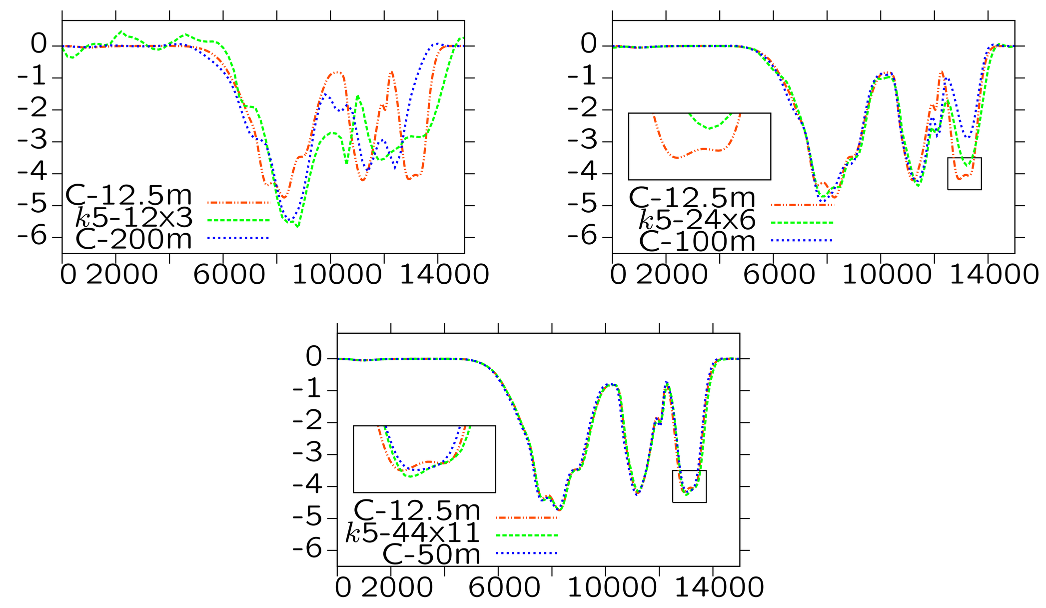

Fig. 6. The potential temperature perturbation in K at height $z = 1\,200$ m after 900 s at different resolutions w.r.t. reference solution (C-200m). Resolutions for the DUNE solutions (k5-12×3, k5-24×6, k5-44×11) has been reduced to match the error of the COSMO solution.

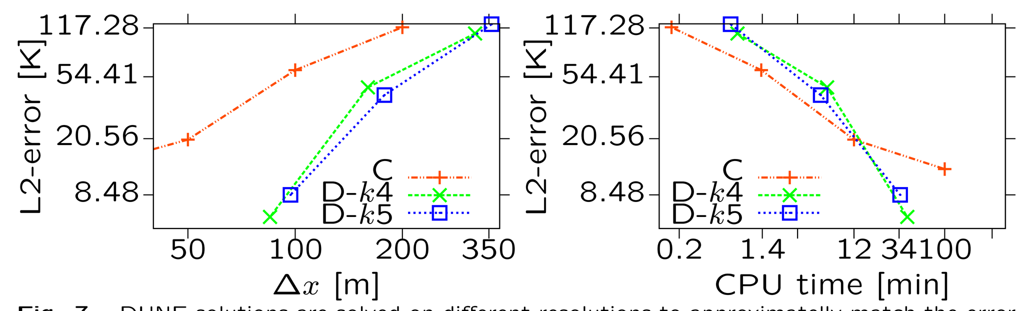

Fig. 7. DUNE solutions are solved on different resolutions to approximately match the error of the COSMO solution on 200, 100, and 50 m.

Inertia-gravity waves

We consider the evolution of a potential temperature deviation from an stably stratified background atmosphere (see [Skamarock and Klemp 94]). The perturbation is so small that the bubble does not have enough buoyancy to rise, but rather oscillates in the vertical direction, while being carried by a constant horizontal mean of 20 m/s.

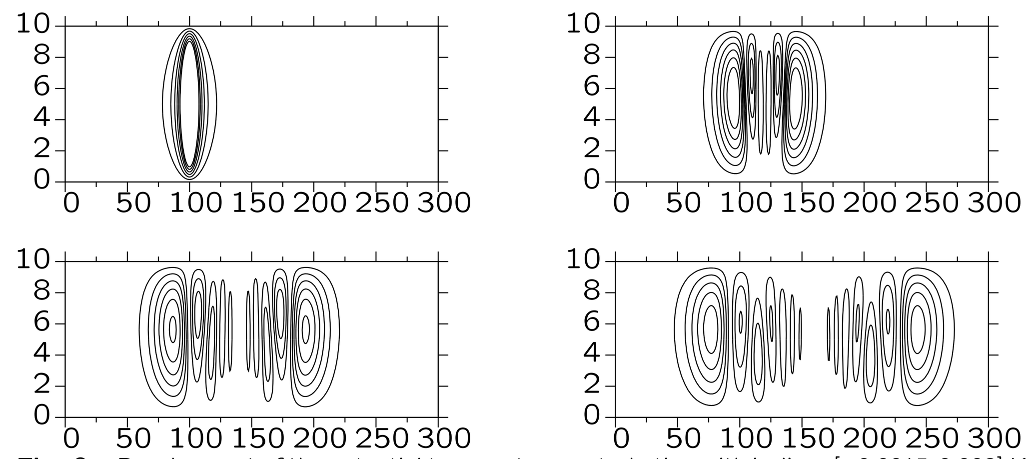

Fig. 8. Development of the potential temperature perturbation with isolines $[-0.0015, 0.003]$ K and CI=0.005 K of the inertia-gravity waves at times $t = 0, 1000, 2000, 3000$ s.

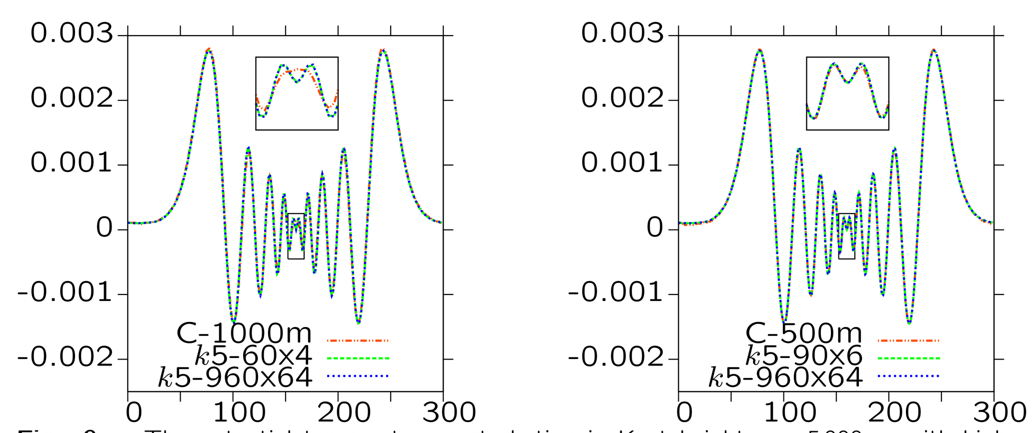

Fig. 9. The potential temperature perturbation in K at height $z = 5\,000$ m with high-resolution solution (k5-960×64), COSMO (C-1000m, C-500m) and DUNE (k5-60×4, k5-90×6).

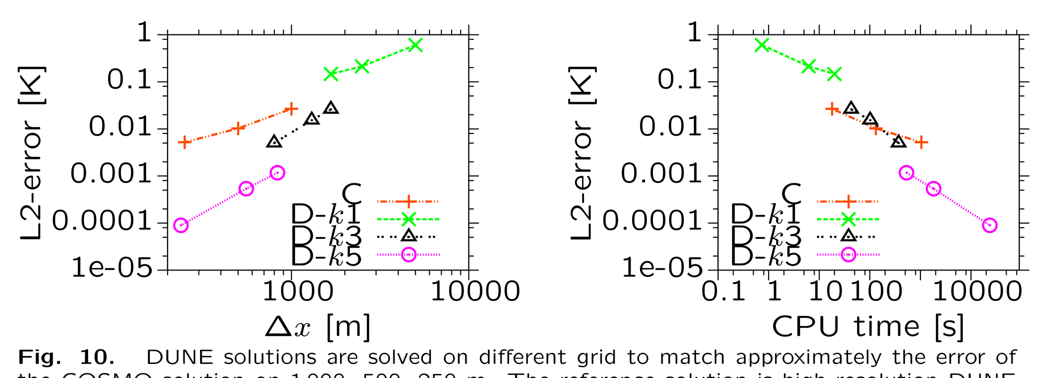

Fig. 10. DUNE solutions are solved on different grid to match approximately the error of the COSMO solution on 1 000, 500, 250 m. The reference solution is high-resolution DUNE k5-960×64.

Conclusions

1. For the same number of stored variables (degrees of freedom for discontinuous Galerkin or points for finite difference) the DUNE core of order at least 3 demonstrates higher subscale resolution than the COSMO core;
2. on the highest resolution prescribed by the test case the DUNE core of order at least 3 is more efficient than the COSMO core;
3. The local conservation and strightforward applicability of the dynamical grid adaptation for the DUNE core have not been considered.

Section of Applied Mathematics
University of Freiburg
Hermann-Herder-Str. 10
D - 79104 Freiburg
Germany

* The author is supported by the priority program MetStröm 1276 of the German Research Foundation (DFG) under keyword "Adaptive numerics for multiscale phenomena".